SDC-91-144

**SDC**
SOLENOIDAL DETECTOR NOTES

# BARREL MUON DETECTOR DESIGN CONSIDERATIONS

January 10, 1990

Jim Wiss
*University of Illinois*

Jim Wiss
University of Illinois
January 10, 1990

# Barrel Muon Detector Design Considerations

This memo summarizes several calculations of momentum resolution for a barrel toroid muon detector. An emphasis is placed on determining the factors necessary to achieve a good $P_\perp$ trigger.

## 1. Preliminaries

Figure 1 shows the efficiency of a muon trigger which demands a muon with a momentum above PTHR as a function of P/PTHR for a muon system capable of offering $\sigma_P/P = 20\%$ , 40 %, and 70 % fractional momentum resolution.

Figure 1 suggests (to me, at least) that a fractional momentum error of $\sigma_P/P = 20\%$ is a reasonable goal for a muon trigger. A 20 % resolution suppresses very low momentum muons at the 5 $\sigma$ level, where as a $\sigma_P/P = 70\%$ detector only suppresses soft muons at the 1.4 $\sigma$ level and thus allows a 7 % trigger efficiency for soft muons.

Toroidal systems will give a nearly constant fractional momentum error until the momentum becomes large enough that finite spacial resolution effects become important. In the absence of special momentum dependent weighting schemes (which presumably reflects the "on - line" situation) the fractional error will follow the form:

$$\frac{\sigma_P}{P} = \sigma_r \sqrt{\left(\frac{P}{P_*}\right)^2 + 1} \tag{1}$$

where $\sigma_r$ is the fractional error at low momenta and $P_*$, which I will call the "effective" momentum, is the momentum beyond which spacial resolution dominates multiple coulomb scattering error (MCS).

For a toroid of length $L$ which is instrumented with N planes evenly spaced throughout the toroid, one can work out analytic simple expressions for the momentum resolution in **one parameter** fits (ie where the incoming direction and position are known from an auxiliary high resolution system (such as the CTD).

$$\sigma_r = \frac{.014}{.3\ B\ \sqrt{L\ X_o}} \sqrt{\frac{130}{81}} \tag{2}$$

$$P_* = .014 \sqrt{\frac{L}{X_o}} \sqrt{N} \left(\frac{L}{\sigma}\right) \sqrt{\frac{13}{162}} \text{ (only for 1 parameter fits!)} \tag{3}$$

The units are GeV - meters - Tesla. These formula give the leading $N$ approximations to the resolution but are fairly accurate once $N$ exceeds 5.

If one considers three parameter fits, where the toroidal system determines the incoming position and angle as well as the momenta, my semi-analytical calculations indicate that the MCS dominated fractional error computed by Eqn. (1) over estimates the 3 parameter fit error by 5%, but the effective momentum gets reduced **by a factor of over 6!** (ie $P_*^{(3\ \mathrm{par})} = 0.159 \times P_*^{(1\mathrm{par})}$). Apart from the constant of Eqn. (3), the prediction that the $P_*$ should be proportional to $\sqrt{N}$ and $\sigma^{-1}$ are well reproduced for my semi-analytic calculations for the case of a three parameter fit.

Figure 2 illustrates spacial resolution effects in the trigger efficiency for the case of a $P_* = 68\ GeV$ , $180\ GeV$ , and $\infty$ for a trigger set at 100 GeV. Figure 2 assumes a low momentum fractional momentum error of 18 %. Poor spacial resolution of the muon toroid read-out planes has its largest effect in prolonging the approach to $\epsilon \rightarrow 1$ at high momentum. Even with a low $P_*$ the trigger is reasonably discriminating against soft muons. One could argue from the clear loss in efficiency up to even 150 GeV in the solid curve ( $P_* = 68\ GeV$ ) that it is highly desirable to keep $P_* > 50\ GeV$ if one is considering triggering thresholds as high as 100 GeV. If one thinks that the maximum triggering threshold would be in vicinity of 50 GeV, a "reasonable" criteria might be to keep $P_* > 25\ GeV$

In conclusion, I believe that a reasonable criteria for a muon system capable of effectively triggering up to 100 GeV , is a low momentum fractional momentum error of about 20 % and an effective momentum of $P_* > 50$ GeV. Once at least a minimal number of read-out planes are instrumented, the fractional momentum error at low momentum is essentially determined by the the thickness and length of the toroid; while the number of read-out planes and their spacial resolution controls the size of $P_*$. If one lowers the triggering threshold, the $P_*$ (but not the $\sigma_r$) criteria could be lowered as well.

## 2. An "HCD" Toroid System

As a starting point, I consider a stand-alone toroid system which follows the rough geometry of the HCD detector. The rough real estate is thus:

**HCD - Toroid**

| Detector | Radius | $\vec{B}$ |
|---|---|---|
| SSD & CTD | 0 m – 2 m | 1.7 T $\hat{z}$ |
| Calorimeter | 2.4 m – 4.8 m | |
| Flux Return | 5 m – 6 m | -.62 T $\hat{z}$ |
| TOROID | 6.5 – 8.0 m | 1.7 T $\hat{\phi}$ |

The solenoidal and flux return fields are essentially irrelevant here since the toroid system only measures trajectories in R-Z plane in my simple stand-alone system.

We begin by considering a system where the toroid is read-out by a read-out plane on its inner radius, outer radius and some number of planes interspersed throughout the toroid. In this stand-alone mode we make no use of any other position measurements from either the beam or chambers not adjacent to the toroid. **The unfortunate aspect of this design**, is at least 3 planes are necessary to fit for the momentum, position, and slope and hence **at least one plane will be have to exist within the toroid** itself. We considered a

design where the detector planes are evenly spaced and have a $\sigma_z$ resolution of $\sigma_z = 400\mu m$. The toroid has a radial extent of 1.5 m and a field of 1.7 T. The following resolution parameters were obtained as the number of planes was varied from 3 (minimal number) to 6.

| $N$ | $\sigma_r$ | $P_*$ |
|---|---|---|
| 3 | 0.20 | 58 GeV |
| 4 | 0.19 | 61 GeV |
| 5 | 0.19 | 67 GeV |

As expected, there is little degradation in the fractional momentum error at low momentum as one decreases the number of planes. The increase in the $P_*$ with increasing number of planes does not appear to warrant anything but a minimal $N = 3$ system.

2.a Use of the Z beam constraint

Perhaps the $Z$ of the beam will be known to $\sigma_z = 5\ mm$ and this information can be used to supplement the momentum resolution of the above system for the use of triggering. A particularly attractive possibility would be to reduce the number of toroid planes to two – one on either side of the toroid– and obtain the necessary third spacial point from the beam.

Figure 3 shows the fractional momentum error as a function of P for a two plane toroid system (with $\sigma_z = 400\mu m$) where we include the beam point with a weight appropriate to $\sigma_z = 5\ mm$. An identical curve is obtained if one employs MCS weighting since there is no "redundant" information in this minimal 2 plane system which can be down weighted. The fractional momentum error at low momentum appears to be unacceptable according to the stated criteria of $\sigma_P/P \leq 20\%$.

Although the beam constraint does not act as a viable alternative to a third plane, will hit help improve momentum resolution to include it in the fit? Figure

4 provides a surprising answer for a 6 plane system. The two solid curves show the fractional momentum error as a function of momentum for fits without special MCS weighting, (ie the points are weighted by the reciprocal of their asymptotic resolution). At low momenta, the fits which use the beam point (with a weight corresponding to $\sigma_z = 5mm$) actually have a fractional momentum error which is twice as poor as a fit which leaves out the beam point at low momentum. Inclusion of the beam point does improves resolution at momenta beyond 100 GeV. The dashed curve shows the fractional momentum error for a fit which includes the beam point and is properly MCS weighted. When properly weighted, the inclusion of the beam position in the fit always improves momentum resolution. Without proper weighting, the inclusion of the beam position actually acts as an information destroyer.

2.b Inclusion of a plane directly before flux return

It is probably possible to include a muon plane at a location right before the flux return and thus have a three plane geometry given below:

**2 + 1 Option**

| Detector | Radius | $\vec{B}$ |
|---|---|---|
| SSD & CTD | 0 m – 2 m | 1.7 T $\hat{z}$ |
| Calorimeter | 2.4 m – 4.8 m | |
| $\mu 1$ | 4.9 m | |
| Flux Return | 5 m – 6 m | -.62 T $\hat{z}$ |
| $\mu 2$ | 6.5 m | |
| TOROID | 6.5 – 8.0 m | 1.7 T $\hat{\phi}$ |
| $\mu 3$ | 8.0 m | |

We can call this deployment the 2 + 1 plane option since the third plane lies outside the toroid.

Figure 5 gives the fractional momentum error as a function of momentum for the above 3 plane system. The solid curve uses just the R-Z view; while the dashed curve uses information from the flux return field as well. The figure assumes that the muon planes have $\sigma_{r\phi} = \sigma_z = 400\mu m$. The $R - \phi$ view provides little additional information. This three plane system has a low momentum fractional momentum error of $\sigma_r = 28\%$ and a large effective momentum of $P_* = 171\ GeV$. Figure 6 compares the efficiency as a function of momentum for a 100 GeV muon trigger for this 2 + 1 plane system and for the previous 3 plane system with the third plane in the middle of the toroid. The 2 + 1 plane trigger will have poorer performance at low momenta than the 3 plane option owing to the larger value of $\sigma_r$. The 2 + 1 option offers only suppresses soft muons on the 3.6 $\sigma$ level. On the other, the 2 + 1 plane trigger comes to asymptotic efficiency above 100 GeV much faster than the 3 plane option owing to its much higher $P_*$. The **big advantage** of the 2+1 option is that one does not have to put a muon plane in the middle of the toroid system to get three spacial coordinates.

The inclusion of an additional plane outside of the toroid does quite a bit to improve momentum resolution. For example, the dashed dotted curve of Figure 5 describes the momentum resolution of the below "2 + 2" option:

**2 + 2 Option**

| Detector | Radius | $\vec{B}$ |
|---|---|---|
| SSD & CTD | 0 m – 2 m | 1.7 T $\hat{z}$ |
| Calorimeter | 2.4 m – 4.8 m | |
| $\mu 1$ | 4.9 m | |
| Flux Return | 5 m – 6 m | -.62 T $\hat{z}$ |
| $\mu 2$ | 6.5 m | |
| TOROID | 6.5 – 8.0 m | 1.7 T $\hat{\phi}$ |
| $\mu 3$ | 8.0 m | |
| Air Gap | 8.0 – 9.5 m | |
| $\mu 4$ | 9.5 m | |

The 2 + 2 option offers a low momentum fractional momentum error of $\sigma_r = 20\%$ and a very large effective momentum of $P_* = 295\ GeV$. We could thus afford to reduce our muon plane resolution requirements to only $\sigma_z = 2000\mu m$ and still match our criteria for $P_* > 50\ GeV$. The 2+2 allows us to meet or exceed our design criteria but requires more radial real estate.

Figure 7 shows the fractional momentum resolution at low momentum as a function of the radius of the outermost plane ($\mu 4$). Again we assume the planes have $\sigma_z = 400\ \mu m$. The dashed curve uses proper MCS weighting, while the solid curve has each point weighted by its inverse asymptotic spacial resolution (ie equal weighting). We note that diminishing returns in reducing $\sigma_r$ beyond 20 cm of additional radius when one uses MCS weighting; while without the use of MCS weighting about a meter of additional radius is necessary to realize the potential of 2 + 2 option (ie a 27 % improvement in momentum resolution).

It should be possible, even at the trigger level, to perform MCS weighting for an assumed fixed momentum which I will call the *weighting* momentum. The idea here is to fit the muon tracks assuming a covariance matrix which reflects

both the intrinsic chamber resolution and smearing due to MCS calculated for tracks with the *weighting* momentum. Fundamentally, the fitting process finds the track curvature (reciprocal momentum) through a linear transformation of the muon chamber coordinates $X_i$ of the form:

$$\frac{1}{P} = \sum_i \rho_i \, X_i$$

where the $\rho_i$ fitting coefficients depend on the weighting scheme (as long as redundant information exists – ie more than three planes). As long as the weighting scheme ($\rho_i$ coefficients) are constant, the resolution on momentum will be of the effective momentum form:

$$\frac{\sigma_P}{P} = \sigma_r \sqrt{\left(\frac{P}{P_*}\right)^2 + 1}$$

Different weighting schemes using different *weighting* momentum will produce different values of $\sigma_r$ and $P_*$. For tracks with momenta close to the *weighting* momentum, the momentum resolution will be optimal; at other momenta the resolution will be non-optimal (possibly much worse than equal weighting).

Figure 7.2 shows a plot of $P_*$ versus $\sigma_r$ for the 2 + 2 option with the outer most chamber at 8.2 m , 8.4 m, and 9.5 m The box illustrates the criteria $\sigma_r < 0.20 \quad , P_* > 50 \; GeV$. In order to exceed the criteria one needs > 20 cm of additional radius for the outer most muon plane and one must use weights appropriate to a low weighting momenta.

Finally we try the possibility of a 3 + 2 option where we have included an additional plane between the toroid and the calorimeter. The geometry is:

**3 + 2 Option**

| Detector | Radius | $\vec{B}$ |
|---|---|---|
| SSD & CTD | 0 m – 2 m | 1.7 T $\hat{z}$ |
| Calorimeter | 2.4 m – 4.8 m | |
| $\mu 1$ | 4.9 m | |
| Flux Return | 5 m – 6 m | -.62 T $\hat{z}$ |
| $\mu 2$ | 6.1 m | |
| Air gap | 6.1 m – 6.5 m | |
| $\mu 3$ | 6.5 m | |
| TOROID | 6.5 – 8.0 m | 1.7 T $\hat{\phi}$ |
| $\mu 4$ | 8.0 m | |
| Air Gap | 8.0 – 8.4 m | |
| $\mu 5$ | 8.4 m | |

Figure 7.4 gives the fractional momentum resolution as a function of momentum for the 2 + 2 option (with the outermost plane at 8.4 m) (curve a) and for the 3 + 2 option described in the above table (curve b). All the curves in Figure 7.4 assume perfect MCS weighting. The improvement between curve a and curve b is rather modest. We note that the 3 + 3 option has removed the steel between 6.1 and 6.5 m over the 3 + 2 option. Much of the improvement in resolution is just due to the removal of this 40 cm of steel as illustrated by the dashed curve d which shows the resolution if $\mu 2$ information is not used in the fit. Finally curve c gives the resolution for the case where $\mu 1$ is absent from the fits which include planes $\mu 2 \rightarrow \mu 5$ only. Clearly $\mu 1$ provides an important lever arm at high momentum but is redundant at low momenta.

2.c Conclusions

It does indeed appear to be able to construct a muon system which uses a 1.5 thick toroid magnetized to 1.7 T and achieve a 20 % $\rightarrow$ 30 % fractional momentum

error which appears adequate for triggering purposes. Such a system requires the construction of three planes to measure the R–Z trajectory of the track. The Z beam constraint does not appear to produce a viable third coordinate without the use of special MCS weighting schemes. All plans we have considered in this section, have two measuring planes which sandwich the toroid. An adequate solution uses a third plane in the center of the toroid and achieves an $\sigma_r = 18\%$ momentum fraction error and $P_* = 68\ GeV$. A barely adequate solution (referred to as a 2 + 1 option) uses a third plane directly after the calorimeter and achieves $\sigma_r = 28\%$ and $P_* = 171\ GeV$. A superior scheme (referred to as the 2 + 2) option uses a fourth plane located after a 1 to 1.5 m air gap after the toroid. The 2 + 2 option achieves $\sigma_r = 20\%$ and $P_* = 295\ GeV$. Because of large $P_*$ values obtained in the 2 + 2 and 2 + 1 option, the muon plane Z resolutions can be considerable relaxed with little harm to the trigger performance. Because of the large differences in MCS environments for the 2 + 2 option planes, considerable improvements are possible if one approachs MCS weighting. It appears that about 40 additional cm for the outermost plane are necessary to realize the potential of the 2 + 2 option if one has $\sigma_z = 400\mu m$ muon plane resolution.

## 3. No Toroid Options

We begin by essentially considering the 2 + 1 option with an un-magnetized absorber. The geometry is thus:

**Un-magnetized 2 + 1 Option**

| Detector | Radius | $\vec{B}$ |
|---|---|---|
| SSD & CTD | 0 m – 2 m | 1.7 T $\hat{z}$ |
| Calorimeter | 2.4 m – 4.8 m | |
| $\mu 1$ | 4.9 m | |
| Flux Return | 5 m – 6 m | -.62 T $\hat{z}$ |
| $\mu 2$ | 6.5 m | |
| ABSORBER | 6.5 – 8.0 m | |
| $\mu 3$ | 8.0 m | |

We assume all 3 planes measure the $R-\phi$ coordinate with 150 $\mu m$ resolution. Momentum dispersion is provided by both the beam constraint and the flux return. Figure 8 shows the fractional momentum error at 10 GeV as a function of the transverse beam error for naively weighted (by asymptotic resolution) (solid) and MCS weighted fits (dashed). Although the beam constraint has the capability of increasing resolution by about 50 % as indicated by the MCS weighted fit, the beam constraint without proper MCS weighting acts as a rather severe information destroyer. We note past a certain point, the resolutions reach a new plateau which indicates that momentum information is coming essentially from the flux return alone. Even with MCS weighting, the 2 + 1 option with a beam constraint does not look capable of meeting the $\sigma_P/P \leq 20\%$ criteria at low momenta.

It may be possible to include information from the outer most CTD plane to further refine the momentum resolution for triggering purposes. The idea here is to use the beam constraint, and a space point at 2 M to obtain a high quality trajectory into the calorimeter and muon steel and use the cruder $R-\phi$ measurements from the 3 planes of the 1 + 2 option to establish the momentum. Figure 9 shows the fractional momentum error for muons at 10 GeV as function

of $\sigma_{R\phi}$ for the outer most plane of the CTC at two meters. We assume a 10 $\mu m$ beam extent and 150 $\mu m$ measurement from the 3 muon planes. Again the solid curve uses naive weighting (asymptotic resolution weighting) and the dashed curve has proper MCS weighting. A 13.5 % low momentum fractional error is possible with a proper weighting scheme as long as better than 1 cm resolution is obtainable by the CTD outermost plane at 2 meters.

Figure 10 gives a $P_*$ versus $\sigma_r$ plot for a cruder system with no muon detector beyond 6.5 m with geometry and resolutions described below:

**Minimal Non-Toroid Option**

| Detector | Radius | $\sigma_{r\phi}$ | $\vec{B}$ |
|---|---|---|---|
| Beam const | 0 | 10 $\mu m$ or 1000 $\mu m$ | |
| outer CTD | 2 m | 400 $\mu m$ | 1.7 T $\hat{z}$ |
| Calorimeter | 2.4 m – 4.8 m | | |
| $\mu 1$ | 4.9 m | 400 $\mu m$ | |
| Flux Return | 5 m – 6 m | | -.62 T $\hat{z}$ |
| $\mu 2$ | 6.5 m | 400 $\mu m$ | |

The solid curve of Figure 10 is for a 10 $\mu m$ beam constraint; the dashed curve is for a 1000 $\mu m$ beam constraint. Clearly a rather crude beam constaint provides sufficient resolution. The plot symbol (single point) is for a 10 $\mu m$ beam constraint with information from the beam constraint the outermost CTD and $\mu 1$ only (hence no redundancy). We note that it is possible to meet the resolution criteria without building muon planes outside of the flux return if one can get information from the outermost layer of CTD.

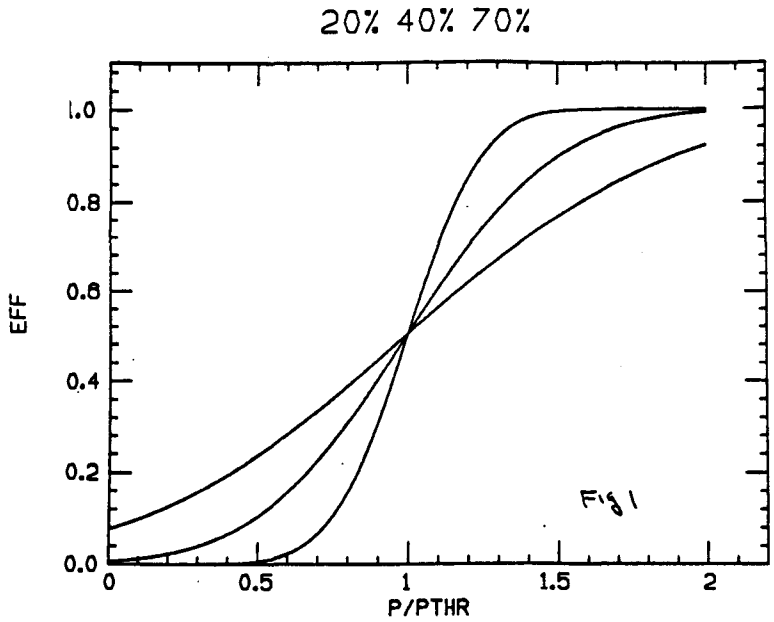
20% 40% 70%
EFF
P/PTHR
Fig 1

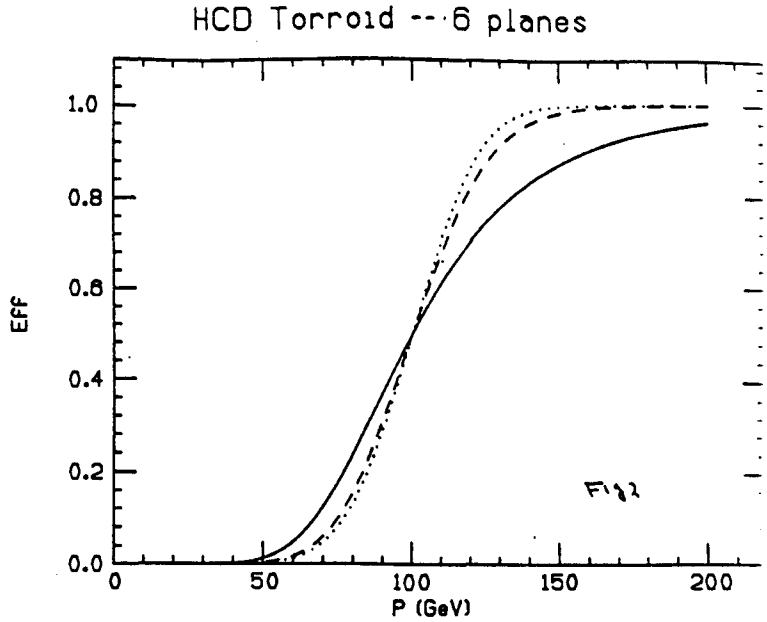
HCD Torroid --- 6 planes
EFF
P (GeV)
Fig 2

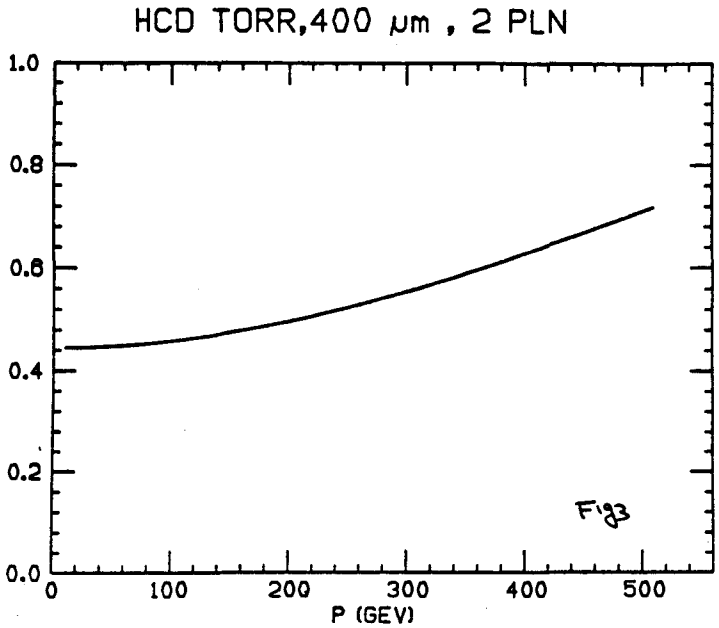
HCD TORR,400 μm , 2 PLN
P (GEV)
Fig 3

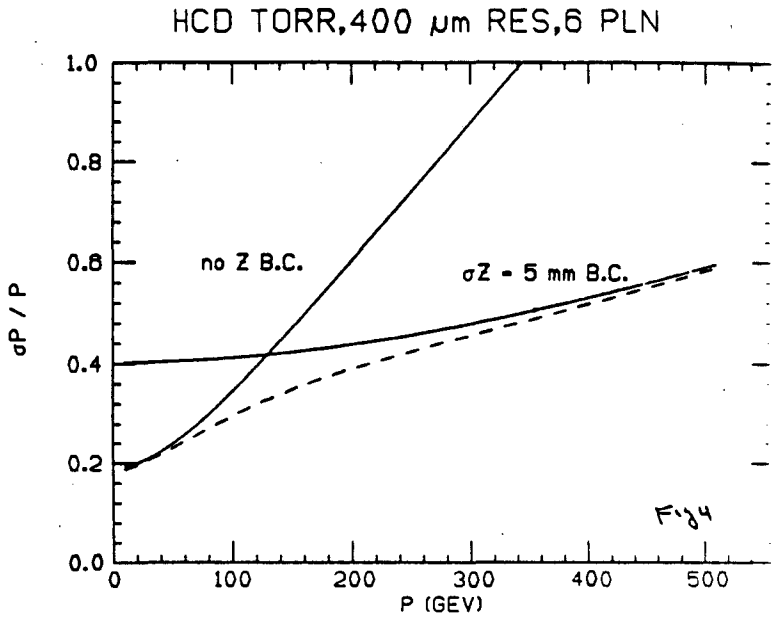
HCD TORR,400 μm RES,6 PLN
σP / P
no Z B.C.
σZ = 5 mm B.C.
P (GEV)
Fig 4

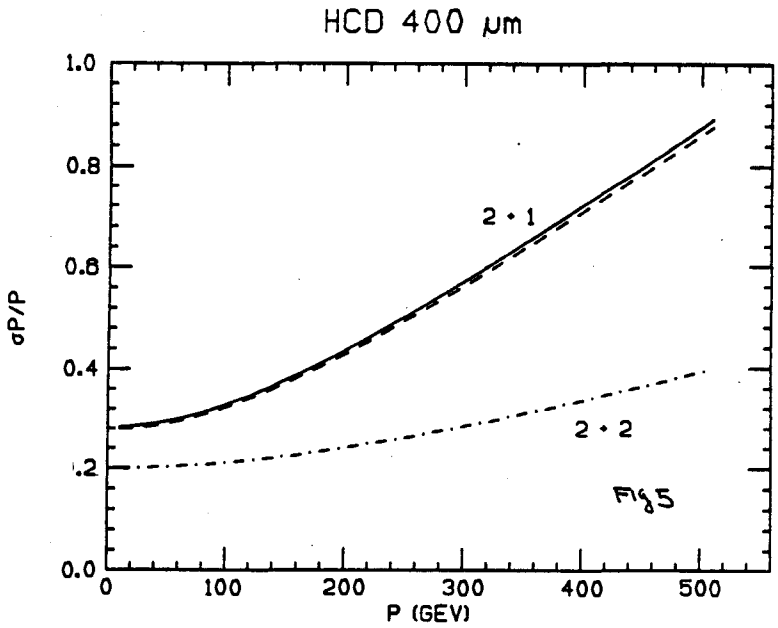
HCD 400 μm
σP/P
2 + 1
2 + 2
P (GEV)
Fig 5

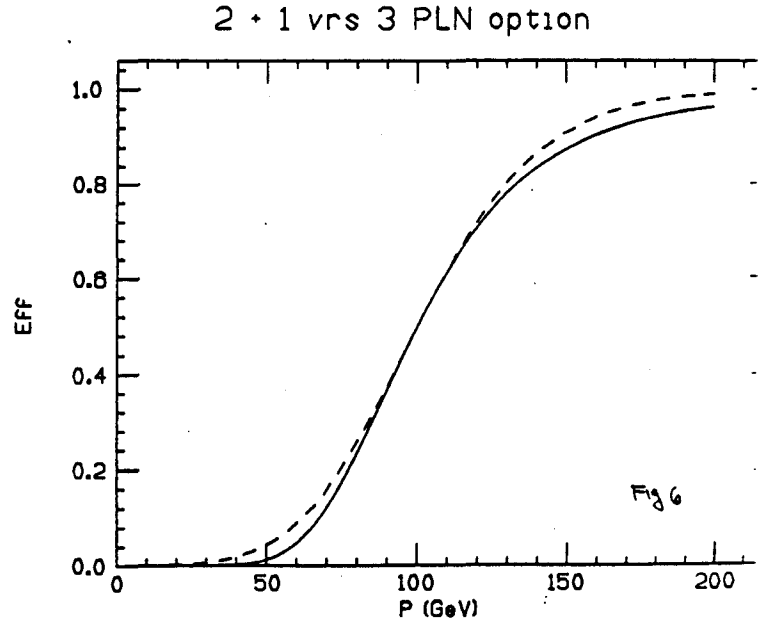
2 + 1 vrs 3 PLN option
EFF
P (GeV)
Fig 6

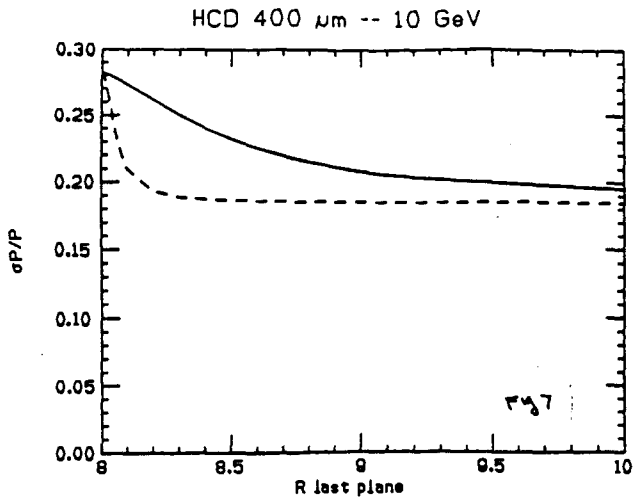
HCD 400 μm -- 10 GeV
σP/P
R last plane
Fig 7

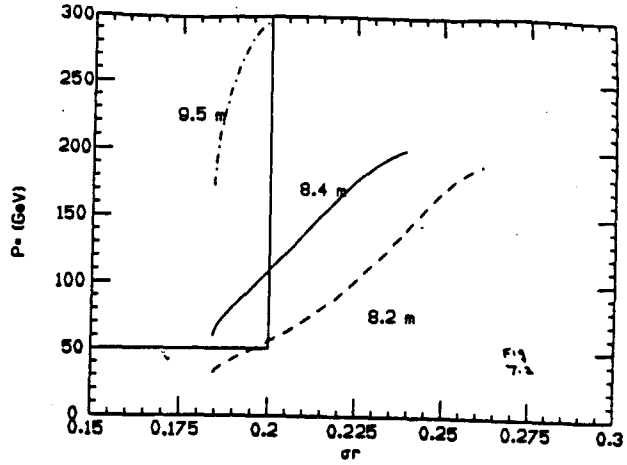
9.5 m
8.4 m
8.2 m
Pe (GeV)
σr

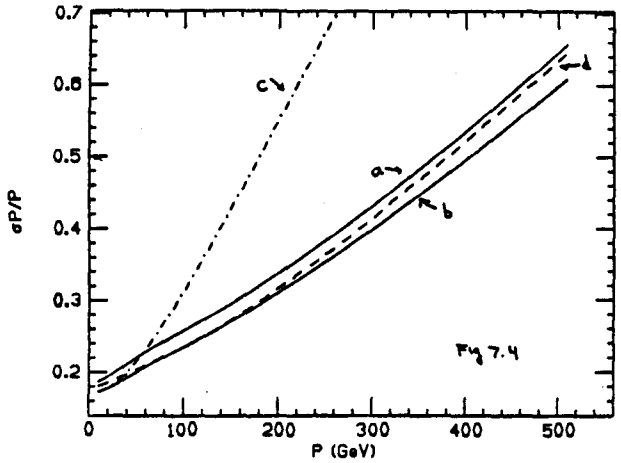
c
a
b
d
σP/P
P (GeV)
Fig 7.4

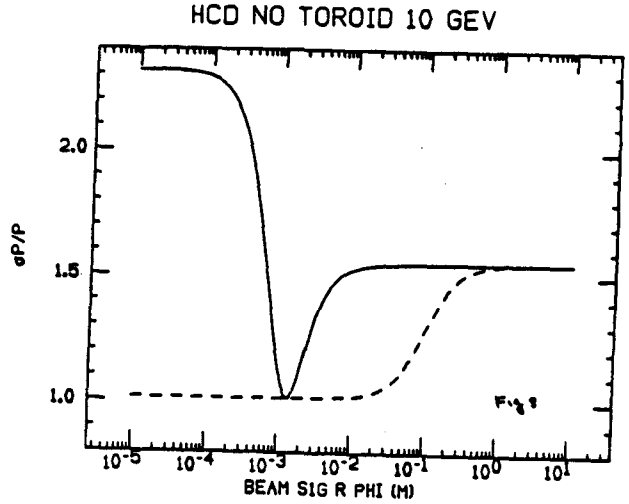
HCD NO TOROID 10 GEV
σP/P
BEAM SIG R PHI (M)

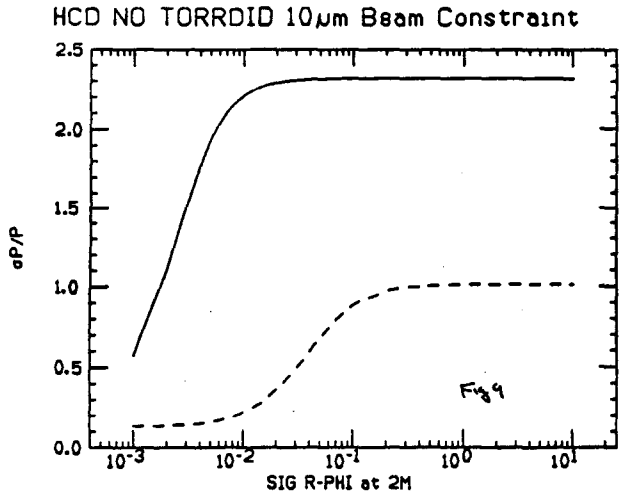
HCD NO TORROID 10μm Beam Constraint
σP/P
SIG R-PHI at 2M
Fig 9

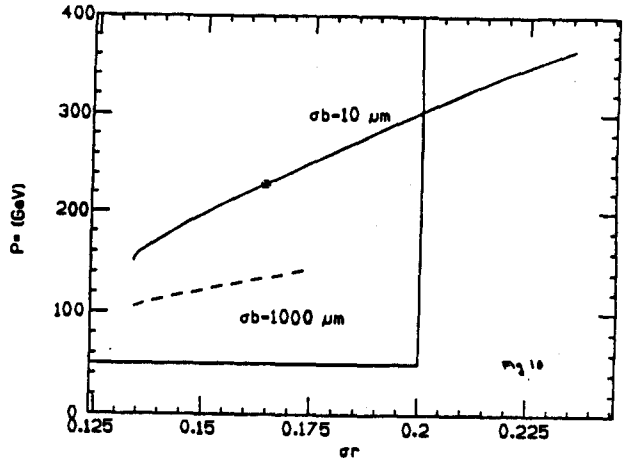
σb-10 μm
σb-1000 μm
Pe (GeV)
σr